ACS APPLIED MATERIALS & INTERFACES

Research Article

www.acsami.org

Preparation and Surface Property of Fluoroalkyl End-Capped Vinyltrimethoxysilane Oligomer/Talc Composite-Encapsulated Organic Compounds: Application for the Separation of Oil and Water

Yuri Oikawa,[†] Tomoya Saito,[†] Satoshi Yamada,[‡] Masashi Sugiya,[‡] and Hideo Sawada*[,†]

[†]Department of Frontier Materials Chemistry, Graduate School of Science and Technology, Hirosaki University, Hirosaki 036-8561, Japan

[‡]Research and Development Division, , Nippon Chemical Industrial Co., Ltd., Koto-ku, Tokyo 136-8515, Japan

ABSTRACT: Fluoroalkyl end-capped vinyltrimethoxysilane oligomer [R_F−$(CH_2$−$CHSi(OMe)_3)_n$−R_F; n = 2, 3; R_F = $CF(CF_3)OC_3F_7$ (R_F−VM oligomer)] can undergo the sol−gel reaction in the presence of talc particles under alkaline conditions at room temperature to provide the corresponding fluorinated oligomeric silica/talc nanocomposites (R_F−VM−SiO_2/Talc). A variety of guest molecules such as 2-hydroxy-4-methoxybenzophenone (HMB), bisphenol A (BPA), bisphenol AF, 3-(hydroxysilyl)-1-propanesulfonic acid (THSP), and perfluoro-2-methyl-3-oxahexanoic acid (R_F−COOH) are effectively encapsulated into the R_F−VM−SiO_2/Talc composite cores to afford the corresponding fluorinated nanocomposites−encapsulated these guest molecules. The R_F−VM−SiO_2/Talc composites encapsulated low molecular weight aromatic compounds such as HMB and BPA can exhibit a superoleophilic−superhydrophobic characteristic on the surfaces; however, the R_F−VM−SiO_2/Talc composite-encapsulated THSP and R_F−COOH exhibit a superoleophobic−superhydrophilic characteristic on the modified surfaces. In these nanocomposites, the R_F−VM−SiO_2/Talc/THSP composites are applicable to the surface modification of polyester fabric, and the modified polyester fabric possessing a superoleophobic−superhydrophilic characteristic on the surface can be used for the membrane for oil (dodecane)/water separation. In addition, the R_F−VM−SiO_2/Talc composites−encapsulated micrometer-size controlled cross-linked polystyrene particles can be also prepared under similar conditions, and the obtained composite white-colored particle powders are applied to the packing material for the column chromatography to separate water-in-oil (W/O) emulsion.

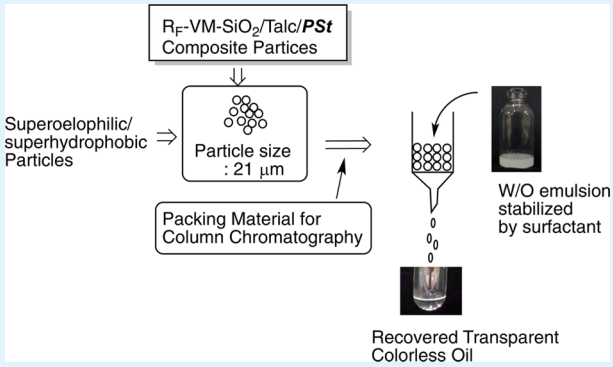

KEYWORDS: *fluorinated oligomer, silica, talc composite, cross-linked polystyrene particle, superhydrophobic−superoleophilic characteristic, superhydrophilic−superoleophobic characteristic, superamphiphobic characteristic, separation of oil/water*

INTRODUCTION

Talc [$Mg_3Si_4O_{10}(OH)_2$] is a hydrated magnesium sheet silicate presenting a lamellar structure, and the lamellar platelets are only held together by van der Waals forces, which leads to talc being a soft mineral, defined as 1 on the Mohs scale.[1−6] From these points of view, talc can be a strong reinforcing filler, and can be useful in a large number of applications in polymers, papers, paints, cosmetics, pharmaceutics and ceramics industries.[7−11] Talc can also provide better dispersion and orientation in the polymer matrix than other fillers because talc platelets are bounded by weak van der Waals forces.[12−15] Addition of talc improves the mechanical properties of the polymer composites, and there have been a variety of reports on the talc-filled polymers such as polypropylene (PP) and poly(lactic acid) (PLA).[16−22] In these talc-filled composites, dry coating of talc particles with fumed silica has been also studied to control their wettability and dispersibility.[23] Hitherto, we have been comprehensively studying on the preparation and properties of fluoroalkyl end-capped oligomers/inorganic nanocomposites by using a wide variety of inorganic nanoparticles such as silica, magnetite, titanium oxide, zinc oxide, gold, copper, silver, calcium carbonate, hydroxyapatite, and calcium silicide.[24−28] These fluorinated nanocomposites can exhibit not only the surface active characteristic imparted by fluorines but also unique properties derived from the inorganic nanoparticles in the composites.[24−28] In these fluorinated nanocomposites, fluoroalkylated vinyltrimethoxysilane oligomer/silica nanocomposites can exhibit the completely superhydrophobic characteristic (water contact angle value: 180°) with good oleophobic property.[29] Calcium silicide fine particles have also been encapsulated into the fluoroalkylated vinyltrimethoxysilane oligomeric silca nanoparticle cores to

Received: February 21, 2015
Accepted: June 4, 2015
Published: June 4, 2015

DOI: 10.1021/acsami.5b01588
ACS Appl. Mater. Interfaces 2015, 7, 13782−13793

provide the superoleophobic−superhydrophilic characteristic on the modified surface.[30] Talc platelets are bounded by weak van der Waals forces, and such interaction enables the talc in the polymer matrices to impart the good dipersibility toward the numerous polymers.[1−9] Thus, it is of particular interest to develop fluoroalkylated oligomeric nanocomposites, especially fluoroalkylated vinyltrimethoxysilane oligomer/inorganic nanocomposites by using talc particles, from the viewpoints of the creation of a variety of surfaces possessing not only superoleophobic−superhydrophilic but also other unique surface active characteristics. Here, we report that fluoroalkylated vinyltrimethoxysilane oligomer can be applicable to the nanocomposite reaction with talc particles, and a variety of guest molecules are smoothly encapsulated into these composite cores. The obtained fluorinated nanocomposites encapsulating these guest molecules can provide the controlled surface active characteristics such as superoleophilic−superhydrophobic, superoleophobic−superhydrophilic, and superamphiphobic characteristics by controlling the structures of these molecules. In contrast, the fluoroalkylated oligomeric silica nanocomposites encapsulated these molecules, which were prepared by using no talc particles, provide the oleophobic−superhydrophobic property on the surface. Fluorinated talc composites encapsulated the micrometer size-controlled cross-linked polystyrene particles and can provide a similar superoleophilic−superhydrophobic characteristic on the modified surface to that of the fluorinated talc nanocomposites-encapsulated low molecular weight aromatic compounds such as 2-hydroxy-4-methoxybenzophenone, and were applied to the packing material for the column chromatography to separate water in oil (W/O) emulsion. These results will be described in this article.

EXPERIMENTAL SECTION

Measurements. Dynamic light scattering (DLS) measurements were measured by using Otsuka Electronics DLS-7000 HL (Tokyo, Japan). Micrometer size-controlled composite particles were measured by using Shimadzu SALD-200 V (Kyoto, Japan). Thermal analyses were recorded on Bruker AXS TG-DTA2000SA differential thermobalance (Kanagawa, Japan). Contact angles were measured using a Kyowa Interface Science Drop Master 300 (Saitama, Japan). Field emission scanning electron micrographs (FE-SEM) were obtained by using JEOL JSM-7000F (Tokyo, Japan). X-ray diffraction (XRD) measurements were performed by the use of Rigaku MiniFlex 600 (Tokyo, Japan). Dynamic force microscope (DFM) was recorded by using SII Nano Technology Inc. E-sweep (Chiba, Japan). Fourier-transform infrared (FT-IR) spectra were recorded using Shimadzu FTIR-8400 FT-IR spectrophotometer (Kyoto, Japan). Optical and fluorescence microscopies were measured by using OLYMPUS Corporation BX51 (Tokyo, Japan). X-ray photoelectron spectroscopy (XPS) measurements were performed by the use of Shimadzu ESCA 3400 (Kyoto, Japan) with the constant pass energy mode (pass 75) in the recorded spectra and C 1s peak at calibrated binding energy: 285 eV as the reference.

Materials. Talc particles were obtained from Asada Milling Co., Ltd. (Tokyo, Japan), and used as received. Perfluoro-2-methyl-3-oxahexanoyl fluoride and 3-(trihydroxysilyl)propane-1-sulfonic acid (THSP) were used as received from Hydrus Chemical Inc. (Tokyo, Japan) and Azmax Co., Ltd. (Chiba, Japan), respectively. Bisphenol A (BPA), 2-hydroxy-4-methoxybenzophenone (HMB), bisphenol AF (BPAF), cross-linked polystyrene particles, and span 80 (sorbitan monooleate) were purchased from Tokyo Chemical Industrial Co., Ltd. (Tokyo, Japan). Perfluoro-2-methyl-3-oxahexanoic acid (bp: 60 °C/10 mm) was prepared by the hydrolysis of perfluoro-2-methyl-3-oxahexanoyl fluoride. Fluoroalkyl end-capped vinyltrimethoxysilane oligomer was prepared according to our previously reported method.[31] Glass plate (borosilicate glass; micro cover glass: 18 × 18 mm) was purchased from Matunami glass Ind. Ltd. (Osaka, Japan) and was used after washing well with 1,2-dichloroethane.

Preparation of Fluoroalkylated Vinyltrimethoxysilane Oligomeric Silica Nanocomposite-Encapsulated Talc Particles (R_F−VM−SiO_2/Talc). A typical procedure for the preparation of R_F−VM−SiO_2/Talc composites is as follows: To methanol solution (5 mL) containing fluoroalkylated vinyltrimethoxysilane oligomer [200 mg; R_F−$[CH_2CHSi(OMe)_3]_n$−R_F; R_F = $CF(CF_3)OC_3F_7$; Mn = 730 (R_F−VM oligomer)] and talc particles (50 mg) was added 25% aqueous ammonia solution (2 mL). The mixture was stirred with a magnetic stirring bar at room temperature for 5 h. Methanol was added to the obtained crude products after the solvent was evaporated off. The methanol suspension was stirred with magnetic stirring bar at room temperature for 1 day. The fluorinated oligomeric silica nanocomposites-encapsulated talc particles were isolated after centrifugal separation for 30 min. The nanocomposite product was washed well with methanol several times and then dried under vacuum at 50 °C for 1 day to afford the expected composites as white powders (168 mg; Scheme 1).

Scheme 1. Preparation of R_F−VM−SiO_2/Talc Composites

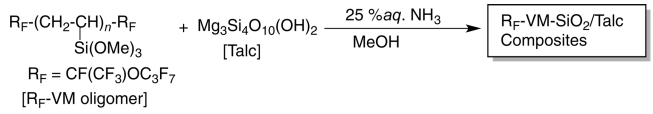

FT-IR spectra (ν/cm^{-1}): R_F−VM−SiO_2/Talc composites, 1334, 1240 (C−F), 1016 (Si−O−Si), 750 (C−C); R_F−VM−SiO_2 oligomeric nanoparticles, 1240, 1199

Preparation of Fluoroalkylated Vinyltrimethoxysilane Oligomeric Silica/Talc Composite-Encapsulated HMB (R_F−VM−SiO_2/Talc/HMB). A 25 % aqueous ammonia solution (2 mL) was added into R_F−VM oligomer (100 mg) methanol (5 mL) solution containing talc particles (250 mg), 2-hydroxy-4-methoxybenzophenone (HMB; 25 mg). The mixture was stirred at room temperature for 5 h. After the removal of the solvent, methanol (25 mL) was added to the isolated composites. The mixture was then stirred for 1 day at room temperature. The expected composite powders were isolated after centrifugal separation for 30 min, and then methanol was used for washing several times. The isolated composite powders were dried under vacuum at 50 °C for 2 days to afford the purified R_F−VM−SiO_2/Talc/HMB nanocomposites (135 mg). The other composite-encapsulated guest molecules were also prepared under similar conditions.

FT-IR Spectra. R_F−VM−SiO_2/Talc/HMB nanocomposites, IR ν/cm^{-1} 1336, 1244 (C−F), 1016 (Si−O−Si), 750 (C−C), 1631 (C═O); R_F−VM−SiO_2/Talc/BPA nanocomposites, IR ν/cm^{-1} 1338, 1244 (C−F), 1016 (Si−O−Si), 750 (C−C), 1612 (C═C); R_F−VM−SiO_2/Talc/BPAF nanocomposites, IR ν/cm^{-1} 1338, 1244 (C−F), 1016 (Si−O−Si), 750 (C−C), 1612 (C═C), 3421 (−OH); R_F−VM−SiO_2/Talc/THSP nanocomposites, IR ν/cm^{-1} 1338, 1244 (C−F), 1016 (Si−O−Si), 750 (C−C), 1199 (S═O), 3524 (−OH); R_F−VM−SiO_2/Talc/R_FCOOH nanocomposites, IR ν/cm^{-1} 1338, 1244 (C−F), 1016 (Si−O−Si), 750 (C−C), 1745 (CO); R_F−VM−SiO_2/Talc/PSt composites, IR ν/cm^{-1} 3024, 2922, 1600 (PSt), 1334, 1240 (C−F), 1008 (Si−O−Si).

Surface modification of glass treated with the R_F−VM−SiO_2/Talc/HMB nanocomposites. The methanol solution (5 mL) containing R_F−VM oligomer [R_F = $CF(CF_3)OC_3F_7$; 200 mg], talc particles (100 mg), HMB (25 mg) and 25% aqueous ammonia solution (2 mL) was stirred with a magnetic stirring bar at room temperature for 5 h. The glass plate was dipped into this solution at room temperature and left for 1 min. These glass plates were lifted from the solutions at a constant rate of 0.5 mm/min and subjected to the treatment for 1 day at room temperature; finally, these were dried under vacuum for 1 day at room temperature. After drying, the contact angles of dodecane and water were measured by the deposit of each droplet (2 μL) on the modified glasses.

DOI: 10.1021/acsami.5b01588
ACS Appl. Mater. Interfaces 2015, 7, 13782−13793

Preparation of the Surfactant-Stabilized Water in Oil (1,2-Dichloroethane) Emulsion. The surfactant (span 80:20 mg) was added into the mixture of water (0.05 mL) and 1,2-dichloroethane (5.0 mL). The expected white-colored W/O emulsion was easily prepared through the ultrasonic irradiation of the obtained mixture for 5 min at room temperature.

RESULTS AND DISCUSSION

Preparation and Properties of R_F−VM−SiO_2/Talc Composites. Fluoroalkylated vinyltrimethoxysilane oligomer (R_F−VM oligomer) was found to undergo the sol−gel reaction in the presence of talc particles under alkaline conditions to provide the corresponding fluorinated oligomeric silica/talc composites [R_F−VM−SiO_2/Talc] in excellent to moderate isolated yields 67−80% (Scheme 1 and Table 1).

Table 1. Preparation of R_F−VM−SiO_2/Talc Composites

run	R_F−VM oligomer (mg)	talc particles (mg)	aq NH_3	yield (%)[a]	contenes of R_F−VM−SiO_2 (%)[b]	size of nanocomposites (nm)[c]
1	200	50	2.0	67	82	108 ± 16
2	200	100	2.0	69	55	94.8 ± 15
3	200	200	2.0	78	42	107 ± 16
4	100	100	2.0	75	36	52.4 ± 5.3
5	50	100	2.0	77	19	41.2 ± 6.1
6	20	100	2.0	80	11	54.9 ± 5.2
7	10	100	2.0	76	5	53.5 ± 3.4
8	5	100	2.0	80	3	62.5 ± 5.4

[a]Yields are based on R_F−VM oligomer and talc particles. [b]Determined by thermogravimetric analyses. [c]Determined by dynamic light scattering (DLS) measurements in methanol.

Table 1 shows that the yields of the R_F−VM−SiO_2/Talc composites are sensitive to the feed ratios of talc and R_F−VM oligomer employed, increasing with greater feed ratios of talc in R_F−VM oligomer−talc. This finding would be due to the smooth encapsulation of talc into the fluorinated oligomeric composite cores under such preparative conditions.

The obtained composites in Table 1 were found to give an extremely poor dispersibility in water; however, these composites afforded good dispersibility and stability in traditional organic solvents such as 1,2-dichloroethane, tetrahydrofuran, methanol, 2-propanol, *N*,*N*-dimethylformamide, dimethyl sulfoxide and fluorinated aliphatic solvents [1:1 mixed solvents (AK-225^{TR}) of 1,1-dichloro-2,2,3,3,3-pentafluoropropane and 1,3-dichloro-1,2,2,3,3-pentafluoropropane]. Thus, we have measured the size of these fluorinated composites in Table 1 in methanol by DLS measurements at 25 °C. Each size of these fluorinated composites is nanometer size-controlled fine particles: 41−108 nm (number-average diameter), as shown in Table 1.

FE-SEM photograph of the R_F−VM−SiO_2/Talc nanocomposites (Run 1 in Table 1) methanol solutions were recorded. The FE-SEM measurements of parent talc particles were also measured under similar conditions, for comparison. These results are shown in Figures 1 and 2.

Electron micrographs show that the shapes of parent talc particles are not uniform owing to their agglomeration (Figure 1). However, interestingly, Figure 2 shows that the uniform R_F−VM−SiO_2/Talc nanocomposite fine particles can be prepared through the sol−gel reaction illustrated in Scheme 1. Electron micrographs of the composites also show the formation of fluorinated composite fine cubic particles with a

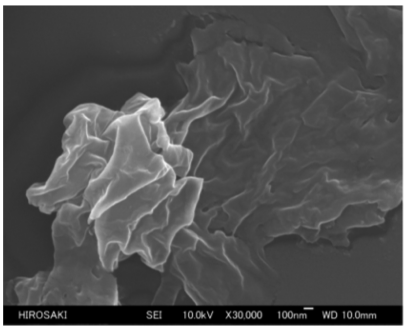

Figure 1. FE-SEM images of parent talc in methanol solution.

mean diameter of 124 nm, and the size (108 nm) determined by DLS was almost the same as to that in FE-SEM measurements.

Thermal stability of the fluorinated nanocomposites in Table 1 was studied by thermogravimetic analyses, in which the weight loss of these composites was measured by raising the temperature around 800 °C (heating rate: 10 °C min^{-1}) in air atmosphere in order to clarify the presence of talc in the composites, and the results are shown in Figure 3.

As shown in Figure 3, the parent R_F−VM−SiO_2 oligomeric nanoparticles, which were prepared by the sol−gel reaction of R_F−VM oligomer under alkaline conditions in Scheme 1, afforded the 74% weight loss around at 530 °C, owing to the partial formation of silica gel during the calcination process. In contrast, the R_F−VM−SiO_2/Talc composites (Runs 1−8 in Table 1) were found to provide the weight loss behavior in proportion to the contents of the R_F−VM−SiO_2 oligomeric nanoparticles in the composites after calcination at 800 °C, and the contents of talc in the composites were estimated to be from 97 to 18%.

XRD spectra of R_F−VM−SiO_2/Talc nanocomposites (Run 4 in Table 1) also show the characteristic peaks related to talc in the nanocomposites, indicating that talc can be encapsulated into fluorinated oligomeric silica nanoparticle cores (Figure 4).

Encapsulation of A Variety of Organic Guest Molecules (Orgs) into the R_F−VM−SiO_2/Talc Nanocomposite Cores. We previously reported that 1,1′-bi(2-naphthol) (BINOL) can be effectively encapsulated into fluoroalkyl end-capped vinyltrimethoxysilane oligomeric nanoparticle cores to provide the corresponding fluorinated oligomeric silica nanocomposite-encapsulated BINOL.[32] Encapsulated BINOL can exhibit the nonflammable property even after calcination at 800 °C.[32] Thus, we tried to encapsulate a variety of organic molecules (Orgs) into the R_F−VM−SiO_2/Talc nanocomposite cores, and the results are shown in Scheme 2 and Table 2.

As shown in Scheme 2 and Table 2, encapsulation of Orgs into the R_F−VM−SiO_2/Talc nanocomposite cores proceeded smoothly to afford the expected fluorinated nanocomposites−encapsulated Orgs [R_F−$(VM−SiO_2)_n$−R_F/Talc/Orgs] in 34−69% isolated yields. The yields of the expected products except for the encapsulation of THSP are sensitive to the feed ratios of Orgs employed, decreasing with greater feed ratios of Orgs from 25 to 200 mg. On the other hand, encapsulation of THSP is not sensitive to the feed ratios of THSP, providing the similar isolated yields in each feed ratio. This finding suggests that guest molecules such as BPA, BPAF, and R_F−COOH should be encapsulated into fluorinated nanocomposite cores through the

DOI: 10.1021/acsami.5b01588
ACS Appl. Mater. Interfaces 2015, 7, 13782−13793

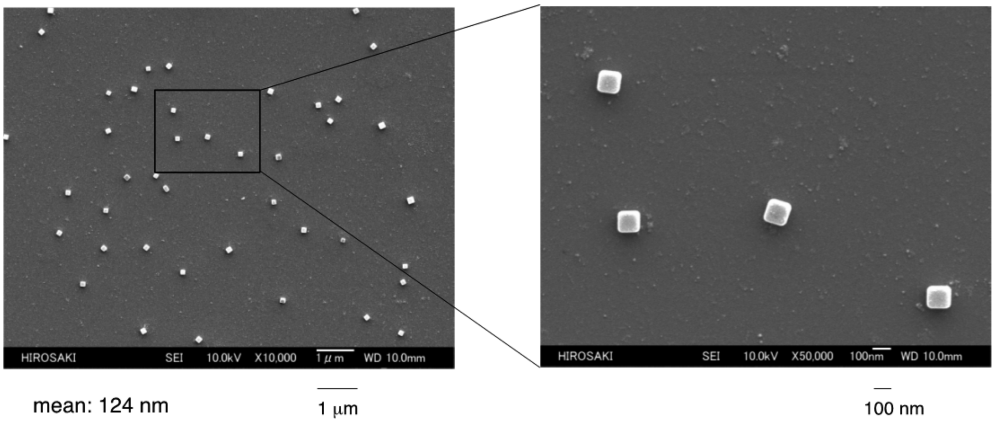

Figure 2. FE-SEM images of R_F–VM–SiO_2/Talc composites in methanol solution (Run 1 in Table 1).

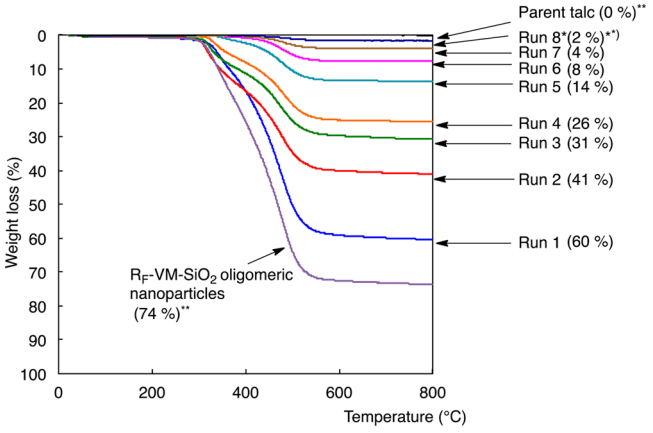

Figure 3. Thermogravimetric analyses of R_F–VM–SiO_2/Talc composites. (*) Run number corresponds to that of Table 1. (**) Weight loss at 800 °C.

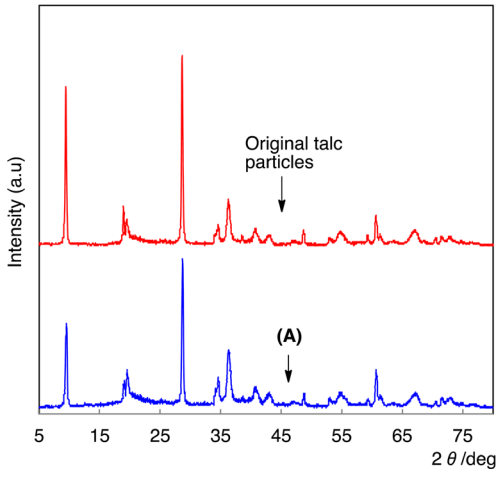

Figure 4. XRD of (A) R_F–VM–SiO_2/Talc composites (Run 4 in Table 1) and original talc particles.

van der Waals interaction; however, THSP should be encapsulated through the chemical reaction between the trimethoxysilyl groups in the oligomer and trihydroxysilyl groups in THSP under alkaline conditions.

The R_F–VM–SiO_2/Talc composites–encapsulated HMB, BPA and BPAF exhibited the similar dispersibility and stability to those of the R_F–VM–SiO_2/Talc composites illustrated in Scheme 1 and Table 1. In contrast, the R_F–VM–SiO_2/Talc composites–encapsulated THSP and R_F–COOH can provide good dispersibility in not only the traditional organic media but also water. This finding is due to the presence of the hydrophilic segments such as sulfo and carboxyl groups in the composites.

We have measured the size of the composites in Table 2 by using DLS measurements, and the results are also summarized in Table 2. The size of these composites are nanometer size-controlled fine particles: 33–117 nm levels. FE-SEM images for the R_F–VM–SiO_2/Talc/HMB and/THSP nanocomposites show that these composites are very fine spherically nanoparticles with mean diameters: 43 and 45 nm, respectively (Figure 5. These composites sizes are quite similar to those (38 and 46 nm) of the DLS measurements in Table 2.

Surface Modification of Glass by Using the R_F–VM–SiO_2/Talc Composites and the R_F–VM–SiO_2/Talc/Orgs Composites. Fluoroalkylated vinyltrimethoxysilane oligomer (R_F–VM oligomer) has been already reported to undergo the sol–gel reaction to afford the corresponding nanoparticles (R_F–VM–SiO_2).[29] The R_F–VM–SiO_2 oligomeric nanoparticles are useful for the surface modification of glass to afford the superhydrophobic property (water contact angle, 180°) with good oleophobicity. The modified glasses were prepared by the treatment with the R_F–VM–SiO_2/Talc composites and R_F–VM–SiO_2/Talc/Orgs composites illustrated in Tables 1 and 2. In addition, we have measured the contact angles of dodecane and water on the modified glass surfaces.

Each R_F–VM–SiO_2/Talc nanocomposite (Runs 1–5 in Table 1) can exhibit the similar contact angles values for dodecane (43–49°) and water (180°) to those (dodecane, 48°; water, 180°) of the parent R_F–VM–SiO_2 oligomeric nanoparticles, although water and dodecane contact angle values on the modified glass surface treated with the parent talc particles were found to become 0° in each case. However, unexpectedly, each R_F–VM–SiO_2/Talc/HMB composite (Runs 1–4 in Table 2) can provide the superoleophilic (dodecane, 0°)–superhydrophobic (water, 180°) characteristic on the modified surfaces. A similar result was obtained in each R_F–VM–SiO_2/Talc/BPA composite illustrated in Runs 5 and 6 in Table 2, suggesting that at the interface with dodecane, hydrophobic fluoroalkyl segments in the composites are replaced by the encapsulated oleophilic HMB or BPA to provide the superoleophilic characteristic. On the other hand, the creation of the superhydrophobic surface (water contact angle, 180°) at the interface with water is due to the smooth replacement from the

DOI: 10.1021/acsami.5b01588
ACS Appl. Mater. Interfaces 2015, 7, 13782–13793

Scheme 2. Preparation of R_F−VM−SiO_2/Talc/Orgs Composites

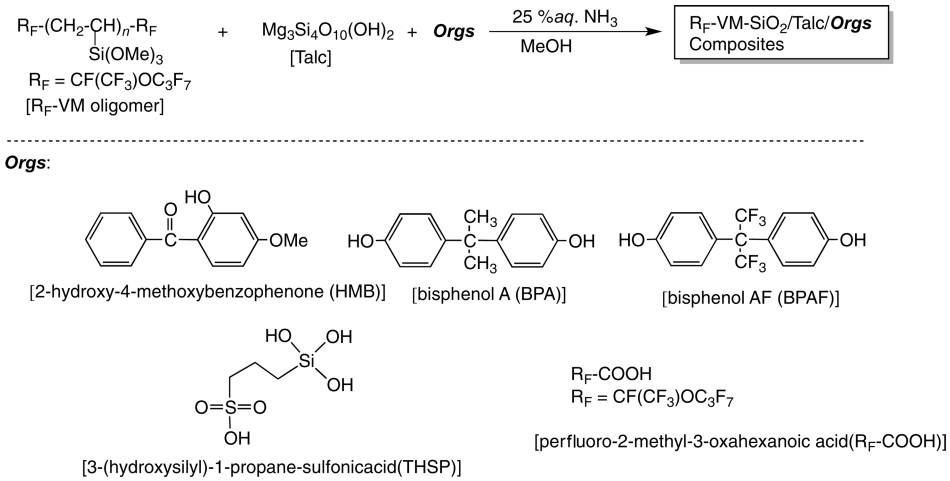

Table 2. Preparation of R_F−VM−SiO_2/Talc/Orgs Composites

run	R_F−VM oligomer (mg)	talc (mg)	aq NH_3 (ml)	Orgs (mg)	yield (%)[a]	size of composites (nm)[b]
			HMB			
1	100	100	2.0	25	60	33.4 ± 7.3
2				50	55	38.2 ± 5.8
3				100	48	38.1 ± 10
4				200	34	34.2 ± 8.2
			BPA			
5	100	100	2.0	25	50	94.8 ± 9.7
6				50	49	53.3 ± 11
			BPAF			
7	100	100	2.0	25	46	46.2 ± 11
8				50	48	79.4 ± 16
9				100	34	52.4 ± 5.4

[a]Yields are based on R_F−VM oligomer and talc particles. [b]Determined by dynamic light scattering (DLS) measurements in methanol.

oleophilic HMB or BPA units in the composites to the hydrophopbic fluoroalkyl groups. Such flip-flop motion between the oleophilic HMB or BPA and the fluoroalkyl groups would be smoothly occurred in the nanocomposite matrices under the environmental change from oil to water on the modified surface. The R_F−VM−SiO_2/Talc/BPAF composites (Runs 7−9 in Table 2) were found to impart the similar oleophobic (dedecane, 35−48°) and superhydrophobic (water, 180°) characteristics to those of the parent R_F−VM−SiO_2/Talc composites, indicating that the encapsulated BPAF should afford the oleophobic characteristic at the interface with dodecane due to the presence of CF_3 units in BPAF.

To further confirm the presence of fluoroalkyl segments and HMB in the nanocomposites to migrate to the surface, giving such superoleophilic−superhydrophobic characteristic, we measured the surface elemental composition by X-ray photoelectron spectroscopy (XPS) using Ar gas ion etching at the conditions of 1−2 kV and 10−20 mA, at which conditions the ion etching rate has been said to be about 5 nm/min. We have shown the binding energies of F_{1s} and C_{1s} for the R_F−VM−SiO_2/Talc/HMB composites (Run 2 in Table 2). The R_F−VM−SiO_2/Talc composites (Run 4 in Table 1) were also studied under the similar conditions, for comparison. These results are shown in Figures 6 and 7.

As shown in Figure 7, the peak intensity of the F_{1s} signal at around 690 eV in the R_F−VM−SiO_2/Talc composites was found to decrease with increasing the etching times (etching conditions; the first time, 1 kV/10 mA for 60 s; the second time, 2 kV/20 mA for 300 s). A similar decrease behavior was observed in the R_F−VM−SiO_2/Talc/HMB composites (Figure 6). On the other hand, the peak intensity of C_{1s} signal at around 287 eV was found to increase with increase of the

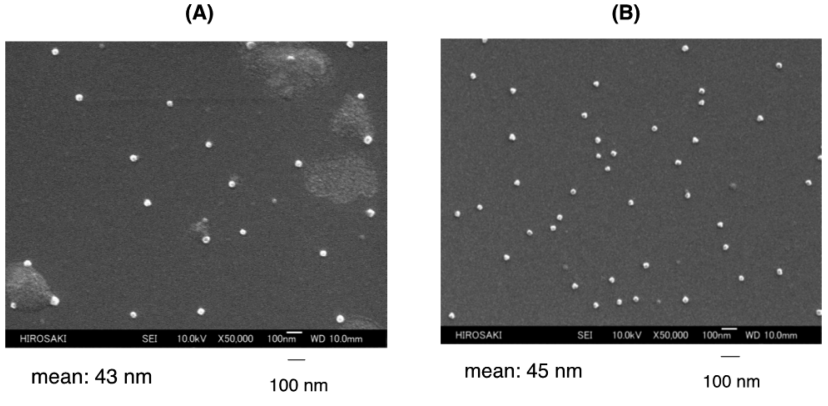

Figure 5. FE-SEM images of (A) R_F−VM−SiO_2/Talc/HMB composites (Run 2 in Table 2) and (B) R_F−VM−SiO_2/Talc/THSP composites (Run 11 in Table 2) in methanol solutions.

DOI: 10.1021/acsami.5b01588
ACS Appl. Mater. Interfaces 2015, 7, 13782−13793

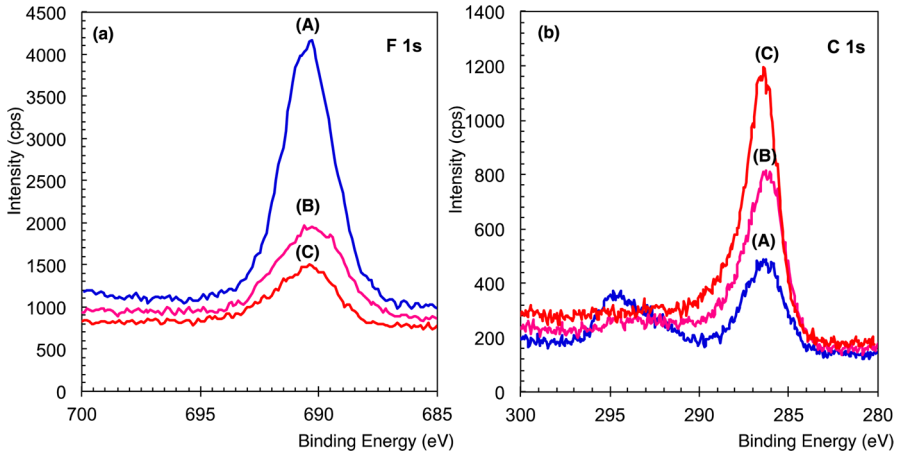

Figure 6. XPS (a) F_{1s} and (b) C_{1s} spectra of R_F−VM−SiO_2/Talc/HMB composites (A) before and after Ar etching (B) the first time and (C) the second time.

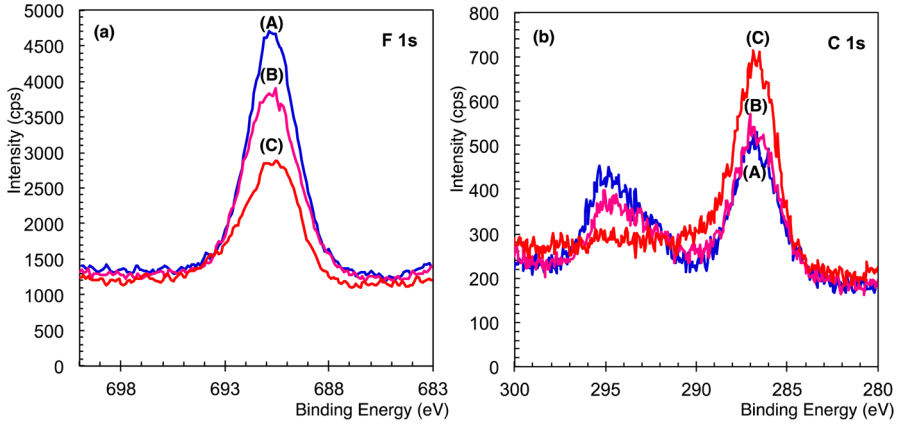

Figure 7. XPS (a) F_{1s} and (b) C_{1s} spectra of R_F−VM−SiO_2/Talc composites (A) before and after Ar etching (B) the first time and (C) the second time.

Table 3. Contact Angles of Water and Dodecane on the Modified Glass Surfaces Treated with R_F−VM−SiO_2/Talc/Orgs Composites (Runs 10−17 in Table 2)

		contact angle (deg)						
		dodecane	water					
			time (min)					
run[a]	feed ratio (R_F−VM oligomer/Talc/Orgs)		0	5	10	15	20	25	30
		Orgs: THSP						
10	100/100/25	83	87	0	*b*			
11	100/100/50	114	69	0	*b*			
12	100/100/100	113	73	0	*b*			
13	100/100/200	93	81	35	0	*b*		
		Orgs: R_F−COOH						
14	100/100/25	111	180	−[b]				
15	100/100/50	118	77	0	*b*			
16	100/100/100	118	108	0	*b*			
17	100/100/200	102	61	0	*b*			

[a]Each run number corresponds to that of Table 2 [b]No change.

etching times. Especially, a more effective increase of the peak intensity of C_{1s} signal after the first etching (Figure 6B) than that of Figure 7B was observed, indicating that the encapsulated HMB in the composites should be arranged regularly on the nanocompsite surface to exhibit the superoleophilic characteristic.

In the case of the R_F−VM−SiO_2/Talc/THSP composites, interestingly, the modified surfaces were found to exhibit not a superoleophilic−superhydrophobic but a superoleophobic−superhydrophilic characteristic as illustrated in Table 3. Because, the contact angle values for dodecane are 83−114°, and the effective decrease of water contact angle values from

DOI: 10.1021/acsami.5b01588
ACS Appl. Mater. Interfaces 2015, 7, 13782−13793

Table 4. Contact Angles of Water and Dodecane on the Modified Glass Surfaces Treated with R_F−VM−SiO_2/Orgs Composites

			contact angle (deg)						
		dodecane	water						
			time (min)						
run	feed ratio (R_F−VM oligomer/Orgs)		0	5	10	15	20	25	30
			Orgs: HMB						
1	100/25	29	140	136	135	134	132	130	129
2	100/50	22	143	138	134	132	129	129	128
3	100/100	27	140	135	134	134	133	129	128
4	100/200	26	138	137	135	135	133	132	131
			Orgs: THSP						
5	100/25	43	149	148	145	143	142	142	141
6	100/50	89	136	133	130	128	128	127	126
7	100/100	94	139	114	109	108	107	106	105
8	100/200	67	79	71	69	64	63	62	59

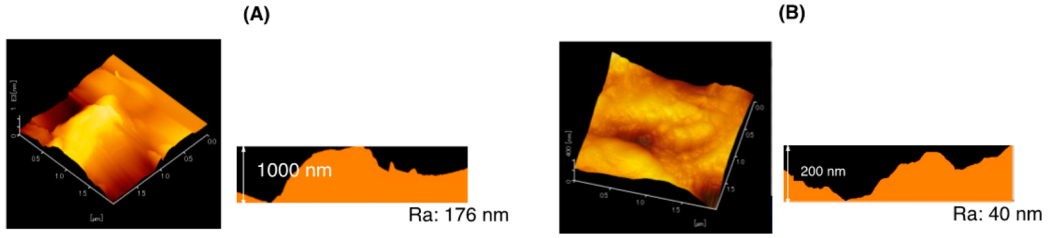

Figure 8. DFM topographic images of the modified glass treated with (A) RF−VM−SiO2/Talc/THSP composites (Run 16 in Table 3) and (B) R_F−VM−SiO_2/Talc composites (Run 1 in Table 3).

69−87° to 0° over only 5 or 10 min was observed in each modified surface (Runs 10−13 in Table 3). The smooth flip-flop motion between hydrophobic fluoroalkyl groups and the hydrophilic sulfo groups in the encapsulated THSP would afford the creation of the superhydrophilic surface at the interface with water. We could have a regular arrangement for the THSP units in the composites at the interface with water. About only 5 or 10 min is needed for the replacement of the fluoroalkyl groups by the THSP units, adapting oneself to the environmental change from air to water.

The R_F−VM−SiO_2/Talc/R_F−COOH composites (Run 14 in Table 3), of whose preparative feed conditions consist of R_F−COOH (25 mg), R_F−VM oligomer (100 mg), and talc (100 mg), can afford the superamphiphobic characteristic (the contact angles for dodecane and water are 111 and 180°, respectively). In contrast, interestingly, the R_F−VM−SiO_2/Talc/R_F−COOH composites (Runs 15−17 in Table 3), of whose preparative feed conditions consist of the higher feed ratios (50−200 mg) of R_F−COOH toward R_F−VM oligomer (100 mg) and talc (100 mg), can provide a superoleophobic−superhydrophilic characteristic (the contact angles for dodecane and water are 102−118 and 0°, respectively). We have observed a remarkable time dependence of the contact angle for water in the R_F−VM−SiO_2/Talc/R_F−COOH composites (Runs 15−17 in Table 3), and the contact angles for water were found to decrease extremely from 108−61 to 0° degree over 5 min to afford the superhydrophilicity on the modified surface, although the corresponding nanocomposites (Run 14 in Table 3), of whose preparative feed conditions consist of the lower feed ratio (25 mg) of R_F−COOH, can provide not superhydrophilic but superhydrophobic property on the surface. The fluoroalkyl segments in the composites are replaced by the hydrophilic carboxyl groups in R_F−COOH when the environment is changed from air to water. The higher feed amounts (50−200 mg) of R_F−COOH in the nanocomposite preparation illustrated in Scheme 2 enable the smooth surface arrangement of the hydrophilic carboxyl groups to provide the completely superhydrophilic surface through the switching behavior between the fluoroalkyl groups and carboxylic segments in the composites.

In this way, we have succeeded in the facile creation of the superoleophlic/superhydrophobic, superoleophobic/superhydrophilic, and superamphiphobic surfaces by using a variety of the R_F−VM−SiO_2/Talc/Orgs composites. To clarify the effect of talc in the composites possessing such surface active characteristics, we measured the dodecane and water contact angle values on the modified glass surface by the treatment of the R_F−VM−SiO_2/Orgs composites (Orgs: HMB and THSP) possessing no talc units, and the results are shown in Table 4.

As shown in Table 4, the R_F−VM−SiO_2/HMB and the R_F−VM−SiO_2/THSP composites can provide the usual oleophobic characteristic (dodecane contact angles, 22−67°) or superoleophobic characteristic (dodecane contact angles, 89 or 94°). However, these modified surface cannot afford the superhydrophobic or superhydrophilic chracteristic, because the water contact angles are 79−149°, and we failed to observe a remarkable time dependence of the contact angles for water to impart the superhydrophilic characteristic.

A lower surface energy and enhancement of the surface roughness are generally very important for creating a highly oleophobic (superoleophobic) surface.[33−40] However, the lower surface tension of oils affords the difficulty to fabricate the superoleophobic surface.[41,42] To verify the creation of the superoleophobic surface, we tried to study on the surface roughness of the modified glass by the treatment of the R_F−VM−SiO_2/Talc/THSP composites (Run 16 in Table 3) by dynamic force microscopy (DFM) measurements. The R_F−VM−SiO_2/Talc composites were also studied under similar

DOI: 10.1021/acsami.5b01588
ACS Appl. Mater. Interfaces 2015, 7, 13782−13793

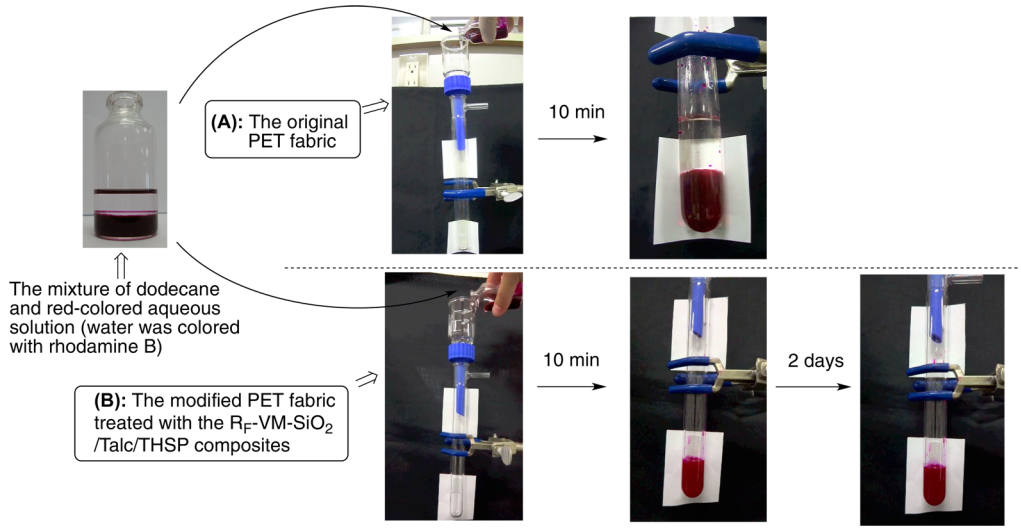

Figure 9. Separation of oil (dodecane)/water (red-colored aqueous solution) by using (A) the original PET fabric and (B) the modified PET fabric treated with the R_F−VM−SiO_2/Talc/THSP composites under atmospheric conditions.

conditions, for comparison. These results are shown in Figure 8.

It was demonstrated that the topographical image of the R_F−VM−SiO_2/Talc/THSP composites surface (Figure 8A) can afford a roughness property, and the roughness average (Ra, 176 nm) obtained from the modified glass surface having the superoleophobic and superhydrophilic characteristics is extremely higher than that (Ra, 40 nm; Figure 9B) of the R_F−VM−SiO_2/Talc composites or that (Ra, 7 nm; data not shown) of the original R_F−VM−SiO_2 oligomeric nanoparticles. This finding suggests that not only talc moiety but also THSP units are very important for the architecture of the rough surface to give the superoleophobic and superhydrophilic surface. Ra values of other R_F−VM−SiO_2/Talc/Orgs composites were measured under similar conditions, and the results are given in Table 5.

Table 5. Ra Values of R_F−VM−SiO_2/Talc/Orgs Composites

Orgs in R_F−VM−SiO_2/talc/Orgs composites	run no. from Table 3	Ra value (nm)
HMB	7	61
BPA	11	56
R_F−COOH	20	78
R_F−VM−SiO_2/Talc composites	1	40
R_F−VM−SiO_2 oligomeric nanoparticles		7

In this way, we verified that such higher Ra values (56−176 nm) than that (40 or 7 nm) of the corresponding R_F−VM−SiO_2/Talc composites or the original R_F−VM−SiO_2 oligomeric nanoparticles are effective to create the superoleophilic/superhydrophobic and superoleophobic/superhydrophilic surfaces.

Application of the R_F−VM−SiO_2/Talc/THSP Composites to the Membrane Materials for Oil/Water Separation. Considerable effort has been recently devoted to the creation of superhydrophilic surface, owing to its high potential applications in numerous fields such as coating technology, including self-cleaning coatings, textile industry, and separation membranes, and much interest has been focused on the randomly fluoroalkylated acrylate copolymers in these fields, especially in the textile industry.[43−47] However, there are some difficulties with removing the oil stain on the traditional superhydrophilic or hydrophilic surfaces due to their easy adhesion of the oils.[48] Therefore, the creation of the superhydrophilic coating surface possessing superoleophobic property would enable the modified polyester (PET) surface to afford the antiadhesion ability. In fact, we have very recently succeeded in the exploration of superoleophobic and superhydrophilic coating surface by the use of perfluoropolyether dicarboxylic acid/silica composites.[49] Thus, we have prepared the modified PET fabric swatch by using the R_F−VM−SiO_2/Talc/THSP composites (Run 11 in Table 2) under the similar dipping technique to those of the glass illustrated in Run 11 in Table 3. It was demonstrated that the dodecane and water contact angle values for the modified PET fabric are 89 and 0°, respectively (we cannot observe the remarkable time dependence for water contact angle), although the parent PET fabric swatch affords no oleophobicity (dodecane contact angle, 0°). This finding suggests that the modified PET surface affords the superoleophobic and superhydrophilic characteristics, quite similar to those of the modified glass surfaces. Such superoleophobic and superhydrophilic characteristics should enable the application of the modified PET fabric swatch to oil−water separation membranes. In fact, the separation of oil (dodecane) and water (water colored red with Rhodamine B) has been studied by the use of this modified fabric as the liquid−liquid separation membrane, and the results are illustrated in Figure 9.

Figure 9B shows that the modified PET fabric is effective for the separation of oil/water under atmospheric conditions, and we can smoothly isolate the red-colored water due to its superhydrophilic/superoleophobic characteristic. The contamination of oil into the aqueous phase was not observed in 10 min or in 2 days, as illustrated in Figure 9B. In contrast, we failed to separate the mixture of oil and water by the use of the nontreated PET fabric under similar conditions as shown in Figure 9A.

Application of the R_F−VM−SiO_2/Talc/PSt Composites to the Packing Materials for Column Chromatography to Separate W/O Emulsion. Hitherto, there have been some reports on the superhydrophobic and superoleophilic coating mesh film and a superhydrophilic and underwater super-

DOI: 10.1021/acsami.5b01588
ACS Appl. Mater. Interfaces 2015, 7, 13782−13793

Scheme 3. Preparation of R_F−VM−SiO_2/Talc/PSt Composites

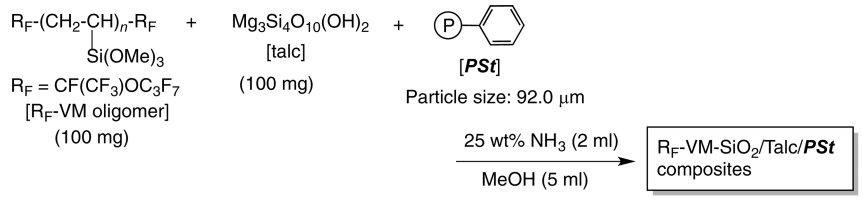

Run	*PSt* (mg)	Yield[a] (%)	Particle size of the composites (μm)
1	25	62	13.8 ± 0.2
2	50	63	20.9 ± 0.5
3	100	71	19.0 ± 0.4
4	200	76	73.4 ± 0.4

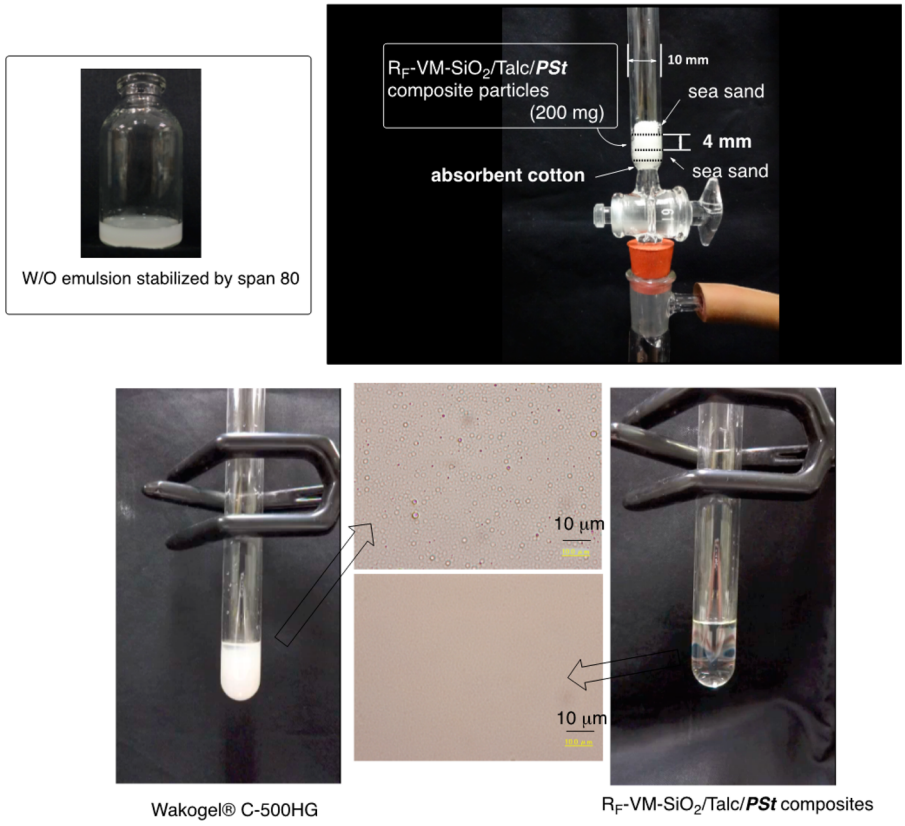

Figure 10. Photographs of (top, right) column chromatography with R_F−VM−SiO_2/Talc/PSt composite particles as a packing material and (left) the W/O emulsion stabilized by span 80 (mixture of 1,2-dichloroethane and water); (bottom) the W/O emulsions after the treatment by the column chromatography by using (left) the Wakogel C-500HG and (right) the R_F−VM−SiO_2/Talc/PSt composites as the packing materials, and (bottom, center) optical microscopy of each eluent.

oleophobic hydrogel-coated mesh for the separation of oil and water.[50,51] Superhydrophilic−superoleophobic materials are also a facile way to realize oil/water separation by either filtration or absorption of oils or water from mixtures selectively.[52,53] In addition, recently, a superhydrophobic−superoleophilic poly(vinylidne fluoride) membrane has been applied to the separation of surfactant-stabilized water-in-oil emulsions.[54] Our present R_F−VM−SiO_2/Talc/Orgs composites are isolated white-colored particle powders. Thus, it is of particular interest to apply these nanocomposite powders to the packing materials for the column chromatography to separate the mixture of oil/water. Usually, silica gel is useful for the packing material for the column chromatography and its average size is around tens of micrometer. We tried to encapsulate the cross-linked polystyrene particles (PSt; average particle size, 92 μm) into the R_F−VM−SiO_2/Talc composite cores due to their application to the packing materials, and the results are shown in Scheme 3.

As shown in Scheme 3, the expected fluorinated composite-encapsulated cross-linked polystyrene particles, R_F−VM−SiO_2/Talc/PSt composites, were obtained in excellent to moderate isolated yields of 62−76%. The average particle sizes of the obtained composites are 14−73 μm, and the higher particle sizes of the composites were obtained by increasing the feed

DOI: 10.1021/acsami.5b01588
ACS Appl. Mater. Interfaces 2015, 7, 13782−13793

amounts of PSt particles from 25 to 200 mg. The smaller size of the composites compared to that of the parent PSt is due to the agglomeration of the used original PSt particles.

We measured the dodecane and water contact angles on the modified glass surface by the treatment of the R_F−VM−SiO_2/Talc/PSt composites in Scheme 3.

Each R_F−VM−SiO_2/Talc/PSt composite shows a superoleophilic−superhydrophobic property on the modified surface because the dodecane and water contact angles are 0 and 180°, respectively. A similar flip-flop motion between the oleophilic PSt moieties and the hydrophobic fluoroalkyl groups to that of the R_F−VM−SiO_2/Talc/HMB composites should easily occur in the composite matrices to provide the superoleophilic−superhydrophobic property on the modified surface.

Thus, we tried to apply the R_F−VM−SiO_2/Talc/PSt composites (Run 2 in Scheme 3) to the packing material for the column chromatography illustrated in Figure 10.

The surfactant (span 80:20 mg)-stabilized water (0.05 mL)-in-oil (1,2-dichloroethane: 5.0 mL) emulsion was prepared under ultrasonic conditions for 5 min at room temperature (Figure 10). The R_F−VM−SiO_2/Talc/PSt composites (particle size, 21 μm; Run 2 in Scheme 3) were applied to the separation of W/O emulsion. As shown in Figure 10, this nanocomposite was effective to separate the fresh W/O emulsion under reduced pressure to isolate the colorless oil (1,2-dichloroethane). Optical micrograph also showed that the water droplet cannot be detected at all in the isolated colorless oil, although we can easily detect the water droplet in the parent W/O emulsion (Figure 10). We tried to study the reusability of the present composite particles as the packing material, and the colorless oil was quantitatively isolated under similar conditions even after using the W/O emulsion three times. In contrast, the silica gel (Wakogel^{TR} C-500HG; average particle size, 22 μm), which is well-known as the packing material, was unable to separate the W/O emulsion under similar conditions (Figure 10).

In this way, our present R_F−VM−SiO_2/Talc/PSt composites are expected to be widely applicable in a variety of fields as the novel packing material for the separation of the mixtures of oil and water.

CONCLUSIONS

R_F−VM−SiO_2/Talc composites were prepared by the sol−gel reaction of the corresponding oligomer in the presence of talc particles under alkaline conditions. The R_F−VM−SiO_2/Talc/Orgs composites were also prepared under the similar sol−gel reactions in the presence of Orgs. R_F−VM−SiO_2/Talc composites were applied to the surface modification of glass to provide the oleophobic−superhydrophobic characteristic on the modified surface. However, the encapsulations of Orgs into the R_F−VM−SiO_2/Talc composite cores can enable the modified glass surfaces to give the controlled wettabilities such as superoleophilic−superhydrophobic, superoleophobic−superhydrophilic, and superamphiphobic characteristics by changing the structures of the encapsulated Orgs. In fact, the encapsulations of low molecular weight aromatic compounds such as HMB and BPA as guest molecules into the fluorinated talc nanocomposite cores can impart the superoleophilic−superhydrophobic surfaces. On the other hand, the encapsulation of THSP and R_F−COOH as guest molecules into the nanocomposite cores can afford the superoleophobic−superhydrophilic surfaces. In the encapsulation of R_F−COOH as a guest molecule, the fluorinated talc nanocomposites, of whose preparative feed conditions consist of the relatively lower feed ratio of R_F−COOH, were found to provide the superamphiphobic property on the surface. The encapsulation of micrometer-size controlled PSt particles into the fluorinated composite cores can also proceed smoothly to afford the corresponding composite-encapsulated PSt particles. These micrometer-size controlled composite particle powders were applied to the packing materials for the column chromatography to separate the W/O emulsion. Recently, there has been a serious problem in increasing environmental pollution, such as the flood of oil in the Gulf of Mexico in 2010.[55] Therefore, not only the R_F−VM−SiO_2/Talc/Orgs composites but also the R_F−VM−SiO_2/Talc/PSt composites have high potential as a wide variety of applicable materials for oil/water separation.

AUTHOR INFORMATION

Corresponding Author

*Tel.: +81-172-39-3947. Fax: +81-172-39-3947 E-mail: hideosaw@hirosaki-u.ac.jp.

Notes

The authors declare no competing financial interest.

REFERENCES

(1) Rayner, J. H.; Brown, G. The Crystal Structure of Talc. *Clays Clay Miner.* **1973**, *21*, 103−114.

(2) Whaling, A.; Bhardwaj, R.; Mohanty, A. K. Novel Talc-Filled Biodegradable Bacterial Polyester Composites. *Ind. Eng. Chem. Res.* **2006**, *45*, 7497−7503.

(3) Ramos, M. A.; Matheu, J. P. V. Effect of Talc Surface Treatment on the Mechanical Properties of Composites based on PP/LDPE Blend Matrices. *Polym. Eng. Sci.* **1991**, *31*, 245−252.

(4) Suh, C. H.; White, J. L. Talc − thermoplastic Compounds: Particle Orientation in Flow and Rheological Properties. *J. Non-Newtonian Fluid Mech.* **1996**, *62*, 175−206.

(5) Mitsuda, T.; Taguchi, H. Formation of Mgnesium Silicate Hydrate and Its Crystallization to Talc. *Cem. Concr. Res.* **1977**, *7*, 223−230.

(6) Douillard, J. M.; Salles, F.; Henry, M.; Malandrini, H.; Clauss, F. Surface Energy of Talc and Chlorite: Comparison between Electronegativity Calculation and Immersion Results. *J. Colloid Interface Sci.* **2007**, *305*, 352−360.

(7) Hargarter, N.; Friedrich, K.; Catsman, P. Mechanical Properties of Glass Fiber/Talc/Polybutylene-terephthalate Composites as Processed by the Radlite Technique. *Compos. Sci. Technol.* **1993**, *46*, 229−244.

(8) Clerc, L.; Feryy, L.; Leroy, E.; Lopez-Cuesta, J.-M. Influence of Talc Physical Properties on the Fire Retarding Behaviour of (Ethylene−Vinyl acetate Copolymer/Magnesium Hydroxide/Talc) Composites. *Polym. Degrad. Stab.* **2005**, *88*, 504−511.

(9) Zhao, G.; Wang, T.; Wang, Q. Studies on Wettability, Mechanical, and Tribological Properties of the Polyurethane Composites Filled with Talc. *Appl. Surf. Sci.* **2012**, *258*, 3557−3564.

(10) Huda, M. S.; Drzal, L. T.; Mohanty, A. K.; Misra, M. The Effect of Silane-Treated and -Untreated Talc on the Mechanical and Physico-mechanical Properties of Poly(lactic acid)/Newspaper Fibers/Talc Hybrid Composites. *Composites, Part B* **2007**, *38*, 367−379.

(11) Huda, M. S.; Drzal, L. T.; Misra, M. A Study on Biocomposites From Recycled Newspaper Fiber and Poly(lactic acid). *Ind. Eng. Chem. Res.* **2005**, *44*, 5593−5601.

(12) Jain, S.; Reddy, M. M.; Mohanty, A. K.; Misra, M.; Ghosh, A. K. A New Biodegradable Flexible Composite Sheet From Poly(lactic acid)/Poly(ε-caprolactone) Blends and Micro-Talc. *Macromol. Mater. Eng.* **2010**, *295*, 750−762.

(13) Leong, Y. W.; Baker, M. B. A.; Ishak, Z. A. M.; Ariffin, A.; Pukanszky, B. Comparison of the Mechanical Properties and Interfacial Interactions Between Talc, Kaolin, and Calcium Carbonate

DOI: 10.1021/acsami.5b01588
ACS Appl. Mater. Interfaces 2015, 7, 13782−13793

Filled Polipropylene Composites. *J. Appl. Polym. Sci.* **2004**, *91*, 3315−3326.
(14) Unal, H. Morphology and Mechanical Properties of Composites Based on Polyamide 6 and Mineral Additives. *Mater. Des.* **2004**, *25*, 483−487.
(15) Murthy, N. S.; Kotliar, A. M.; Sibilia, J. P.; Sacks, W. Structure and Properties of Talc-Filled Polyethylene and nylon 6 Films. *J. Appl. Polym. Sci.* **1986**, *31*, 2569−2582.
(16) Garcia-Martinez, J. M.; Laguna, O.; Areso, S.; Collar, E. P. Polypropylene/Talc Composites Modified by A Succinyl-Fluorescein Grafted Atactic Polypropylene: A Thermal and Mechanical Study Under Dynamic Conditions. *J. Polym. Sci., Part B: Polym. Phys.* **2002**, *40*, 1371−1382.
(17) Lapcik, L., Jr.; Jindrova, P.; Lapcikova, B.; Tamblyn, R. Effect of The Talc Filler Content on The Mechanical Properties of Polypropylene Composites. *J. Appl. Polym. Sci.* **2008**, *110*, 2742−2747.
(18) Duquesne, S.; Samyn, F.; Bourbigot, S.; Amigouet, P.; Jouffret, F.; Shen, K. Influence of Talc on the Fire Retardant Properties of Highly Filled Intumescent Polypropylene Composites. *Polym. Adv. Technol.* **2008**, *19*, 620−627.
(19) Wang, K.; Bahlouli, N.; Addiego, F.; Ahzi, S.; Remond, Y.; Ruch, D.; Muller, R. Effect of Talc Content on the Degradation of Re-extruded Polypropylene/Talc Composites. *Polym. Degrad. Stab.* **2013**, *98*, 1275−1286.
(20) Alonso, M.; Velasco, J. Z.; Velasco, J. Z.; de Saja, J. A. Constrained Crystallication and Activity of Filler in Surface Modified Talc Polypropylene Composites. *Eur. Polym. J.* **1997**, *33*, 255−262.
(21) Qin, Y.; Yang, J.; Yuan, M.; Xue, J.; Chao, J.; Wu, Y.; Yuan, M. Mechanical, Barrier, and Thermal Properties of Poly(lactic acid)/Poly(Trimethylene Carbonate)/Talc Composite Films. *J. Appl. Polym. Sci.* **2014**, DOI: 10.1002/APP.40016.
(22) Fowlks, A. C.; Narayan, R. The Effect of Maleated Polylactic Acid (PLA) as an Interfacial Modifier in PLA-Talc Composites. *J. Appl. Polym. Sci.* **2010**, *118*, 2810−2820.
(23) Lefebvre, G.; Galet, L.; Chamayou, A. Dry Coating of Talc Particles with Fumed Silica: Influence of the Silica Concentratin on the Wettability and Dispersibility of the Composite Particles. *Powder Technol.* **2011**, *208*, 372−377.
(24) Sawada, H. Fluorinated Peroxides. *Chem. Rev.* **1996**, *96*, 1979−1808.
(25) Sawada, H. Synthesis of Self-Assembled Fluoroalkyl End-Capped Oligomeric Aggregates-Applications of These Aggregates to Fluorinated Oligomeric Nanocomposites. *Prog. Polym. Sci.* **2007**, *32*, 509−533.
(26) Sawada, H. Preparation and Applications of Novel Fluoroalkyl End-Capped Oligomeric Nanocomposites. *Polym. Chem.* **2012**, *3*, 46−65.
(27) Sawada, H.; Kikuchi, M.; Nishida, M. Low Molecular Weight Aromatic Compunds Possessing a Nonflammable Characteristic in Fluoroalkyl End-Capped Acrylic Acid Oligomer/Silica Nanocomposite Matrices after Calcination at 800 °C under Atomospheric Conditions. *J. Polym. Sci., Part A: Polym. Chem.* **2011**, *49*, 1070−1078.
(28) Sawada, H.; Tashima, T.; Nishiyama, Y.; Kikuchi, M.; Kostov, G.; Goto, Y.; Ameduri, B. Iodine Transfer Terpolymerization of Vinylidene Fluoride, α-Trifluoromethacrylic Acid and Hexafluoropropylene for Exceptional Thermostable Fluoropolymers/Silica Nanocomposites. *Macromolecules* **2011**, *44*, 1114−1124.
(29) Sawada, H.; Suzuki, T.; Takashima, H.; Takishita, K. Preparation and Properties of Fluoroalkyl End-Capped Vinyltrimethoxysilane Oligomeric Nanoparticels—A New Approach to Facile Creation of a Completely Superhydrophobic Coating Surface with These Nanoparticles. *Colloid Polym. Sci.* **2008**, *286*, 1569−1574.
(30) Saito, T.; Tsushima, Y.; Sawada, H. Facile Creation of Superoleophobic and Superhydrophilic Surface by Using Fluoroalkyl End-Capped Vinyltrimethoxysilane Oligomer/Calcium Silicide Nanocomposites—Development of These Naocomposites to Environmental Cyclical Type-Fluorine Recycle through Formation of Calcium Fluoride. *Colloid Polym. Sci.* **2015**, *293*, 65−73.
(31) Sawada, H.; Nakayama, M. Synthesis of Fluorine-Containing Organosilicon Oligomers. *J. Chem. Soc., Chem. Commun.* **1991**, 677−678.
(32) Sawada, H.; Matsuki, Y.; Goto, Y.; Kodama, S.; Sugiya, M.; Nishiyama, Y. Preparation of Novel Fluoroalkyl End-Capped Trimethoxyvinylsilane Oligomeric Nanoparticle-Encapsulated Binaphthol: Encapsulated Binaphthol Remaining Thermally Stable Even at 800 °C. *Bull. Chem. Soc. Jpn.* **2010**, *83*, 75−81.
(33) Yao, X.; Song, Y.; Jiang, L. Applications of Bio-Inspired Special Wettable Surfaces. *Adv. Mater.* **2011**, *23*, 719−734.
(34) Sunny, S.; Vogel, N.; Howell, C.; Vu, T. L.; Aizenberg, J. Lubricant-Infused Nanoparticulate Coating Assembled by Layer-by-Layer Deposition. *Adv. Funct. Mater.* **2014**, *24*, 6658−6667.
(35) Mertaniemi, H.; Jokinen, V.; Sainiemi, S.; Franssila, A.; Marmur, O.; Ikkala, O.; Ras, R. H. A. Superhydrophobic Tracks for Low-Friction, Guided Transport of Water Droplets. *Adv. Mater.* **2011**, *23*, 2911−2914.
(36) Feng, J.; Huang, B.; Zhong, M. Fabrication of Superhydrophobic and Heat-Insulating Antimony Doped Tin Oxide/Polyurethane Films by Cast Replica Micromolding. *J. Colloid Interface Sci.* **2009**, *336*, 268−272.
(37) Wang, H.; Zhou, H.; Gestos, A.; Fang, J.; Lin, T. Robust, Superamphiphobic Fabric with Multiple Self-Healing Ability Against Both Physical and Chemical Damages. *ACS Appl. Mater. Interfaces* **2013**, *5*, 10221−10226.
(38) Hsu, S.-H.; Chang, Y.-L.; Tu, Y.-C.; Tsai, C. M.; Su, W.-F. Omniphobic Low Moisture Permeation Transparent Polyacrylate/Silica Nanocomposite. *ACS Appl. Mater. Interfaces* **2013**, *5*, 2991−2998.
(39) Lee, S. G.; Ham, S. S.; Lee, D. Y.; Bong, H.; Cho, K. Transparent Superhydrophobic/Translucent Superamphiphobic Coatings Based on Silica-Fluoropolymer Hybrid Nanoparticles. *Langmuir* **2013**, *29*, 15051−15057.
(40) Goto, Y.; Takashima, H.; Takishita, K.; Sawada, H. Creation of Coating Surfaces Possessing Superhydrophobic and Superoleophobic Characteristics with Fluoroalkyl End-Capped Vinyltrimethoxysilane Oligomeric Nanocomposites Having Biphenylene Segments. *J. Colloid Interface Sci.* **2011**, *362*, 375−381.
(41) Tsujii, K.; Yamamoto, T.; Onda, T.; Shibuichi, S. Super Oil-Repellent Surfaces. *Angew. Chem., Int. Ed. Engl.* **1997**, *36*, 1011−1012.
(42) Shibuichi, S.; Yamamoto, T.; Onda, T.; Tsujii, K. Super Water- and Oil-Repellent Surfaces Resulting from Fractal Structure. *J. Colloid Interface Sci.* **1998**, *208*, 287−294.
(43) An, Q.; Xu, W.; Hao, L.; Huang, L. Cationic Fluorinated Polyacrylate Core-Shell Latex with Pendant Long Chain Alkyl: Synthesis, Film Morphology, and Its Performance on Cotton Substrates. *J. Appl. Polym. Sci.* **2013**, *127*, 1519−1526.
(44) Furukawa, Y.; Kotera, M. Water and Oil Repellency of Polysiloxanes with Highly Fluorinated Alkyl Side Chains. *J. Appl. Polym. Sci.* **2003**, *87*, 1085−1091.
(45) Ceria, A.; Hauser, P. J. Atmospheric Plasma Treatment to Improve Durability of a Water and Oil Repellent Finishing for Acrylic Fabrics. *Surf. Coat. Technol.* **2010**, *204*, 1535−1541.
(46) Yang, J.; Song, H.; Yan, X.; Tang, H.; Li, C. Superhydrophilic and Superoleophobic Citosan-based Nanocomposite Coatings for Oil/Water Separation. *Cellulose* **2014**, *21*, 1851−1857.
(47) Ye, H.; Li, Z.; Chen, G.; Fan, D. Synthesis of Bis(1*H*,1*H*,2*H*,2*H*-perfluorooctyl)methylenesuccinate Copolymers and Their Application on Cotton Fabrics. *J. Appl. Polym. Sci.* **2013**, *127*, 402−409.
(48) Liu, K.; Tian, Y.; Jiang, L. Bio-Inspired Superoleophobic and Smart Materials: Design, Fabrication, and Application. *Prog. Mater. Sci.* **2013**, *58*, 503−564.
(49) Sumino, E.; Saito, T.; Noguchi, T.; Sawada, H. Facile Creation of Superoleophobic and Superhydrophilic Surface by Using Perfluoropolyether Dicarboxylic Acid/Silica Nanocomposites. *Polym. Adv. Technol.* **2015**, *26*, 345−352.
(50) Xue, Z. X.; Wang, S. T.; Lin, L.; Chen, L.; Liu, M. J.; Feng, L.; Jiang, L. A Novel Superhydrophilic and Underwater Superoleophobic

DOI: 10.1021/acsami.5b01588
ACS Appl. Mater. Interfaces 2015, 7, 13782−13793

Hydrogel-Coated Mesh for Oil/Water Separation. *Adv. Mater.* **2011**, *23*, 4270−4273.
(51) Gui, X. C.; Wei, J. Q.; Wang, K. L.; Cao, A. Y.; Zhu, H. W.; Jia, Y.; Shu, Q. K.; Wu, D. H. Carbon Nanotube Sponges. *Adv. Mater.* **2010**, *22*, 617−621.
(52) Zhang, J.; Seeger, S. Polyester Materials with Superwetting Silicone Nanofilaments for Oil/Water Separation and Selective Oil Absorption. *Adv. Funct. Mater.* **2011**, *21*, 4699−4704.
(53) Wang, C. X.; Yao, T. J.; Ma, C.; Fan, Z. X.; Wang, Z. Y.; Cheng, Y. R.; Lin, Q. Filter Paper with Selective Absorption and Separation of Liquids that Differ in Surface Tension. *ACS Appl. Mater. Interfaces* **2009**, *1*, 2613−2617.
(54) Zhang, W.; Shi, Z.; Zhang, F.; Liu, X.; Jin, J.; Jiang, L. Superhydrophobic and Superoleophilic PVDF Membranes for Effective Separation of Water-in-Oil Emulsions with High Flux. *Adv. Mater.* **2013**, *25*, 2071−2076.
(55) Allan, S. E.; Smith, B. W.; Anderson, K. A. Impact of the Deepwater Horizon Oil Spill on Bioavailable Polycyclic Aromatic Hydrocarbons in Gulf of Mexico Coastal Waters. *Environ. Sci. Technol.* **2012**, *46*, 2033−20.

DOI: 10.1021/acsami.5b01588
ACS Appl. Mater. Interfaces 2015, 7, 13782−13793